Progress In Electromagnetics Research, PIER 45, 217–241, 2004

PENETRATION BY A LASER-LIGHT INDUCED FIELD AND COUPLING TO A MONOPOLE ATTACHED ON AXIS TO A BODY OF REVOLUTION

C. Ozzaim

Department of Electrical Engineering
Dumlupinar University
Tavsanli yolu 10.km Kutahya, 43100 Turkiye

C. M. Butler

Department of Electrical and Computer Engineering
Clemson University
Clemson, SC 29634-0915, USA

Abstract—In this paper is presented a method for computing, and an experimental procedure for verifying, the coupling of a signal, caused by a modulated laser beam, to a load impedance terminating a coaxial waveguide whose center conductor protrudes into a an open-ended body of revolution (BOR). The excitation is the signal radiated by electrons emitted from the conducting surface by an impinging laser beam, modulated in such a way that the electrons escaping the surface oscillate harmonically in time causing them to radiate a coherent signal at an angular frequency ω. For a vanishingly small spot of laser light on the conducting surface, the radiating source is modeled as an electric dipole normal to and located at the surface. To perform this computation directly is very difficult so we resort to an indirect method that allows us to realize significant savings with no loss in generality. The indirect approach adopted here takes the advantage of the reciprocity and allows one to determine the received signal at the coax terminal load from knowledge of the field radiated by a small wire probe mounted on the symmetry axis of the BOR under the condition that the excitation results from a current generator impressed at the terminal end of the coax. This scheme necessitates the formulation and solution of a simpler integral equation. In principle, the approach developed to solve this problem is exact and rigorous. The validity of this approach is demonstrated numerically and experimentally.

1. INTRODUCTION

Electromagnetic penetration into a shielded enclosure and coupling to a receiver inside the shield where the coupling path is produced by a center-fed dipole antenna and coaxial transmission line system has been studied and reciprocity has been used to relate the electric field incident on the antenna to the short circuit current in the transmission line [1]. The electromagnetic field received by a thin-wire probe mounted on the nose of a missile like body of revolution (BOR) has been studied and the signal coupled to the coaxial transmission line has been determined from the far zone field pattern and reciprocity theorem [2]. The application of reciprocity has also been presented for computing, the coupling of a signal, caused by an elementary electric dipole, to a load impedance terminating a coaxial transmission line whose center conductor protrudes into an open-ended cylindrical tube [3]. In this paper, reciprocity method is presented for computing, and an experimental procedure for verifying, the coupling of a signal, caused by a modulated laser beam, to a load impedance terminating a coaxial waveguide whose center conductor protrudes into a an open-ended body of revolution (BOR) as illustrated in Fig. 1. The BOR is a right circular cylindrical shell with a planar bottom through which protrudes the center conductor of a coax. For convenience, we refer to the structure as a "can" connected to a loaded coaxial monopole. The can wall and bottom are taken to be vanishingly thin perfectly conducting, as are the inner and outer walls of the coaxial waveguide. The coax axis is the same as the cylinder axis and its outer conductor terminates at, and is electrically connected to, the can bottom. The excitation is the signal radiated by electrons emitted from the conducting surface by an impinging laser beam, modulated in such a way that the electrons escaping the surface oscillate harmonically in time causing them to radiate a coherent signal at an angular frequency ω. The laser-excited electrons radiate in the presence of the can and

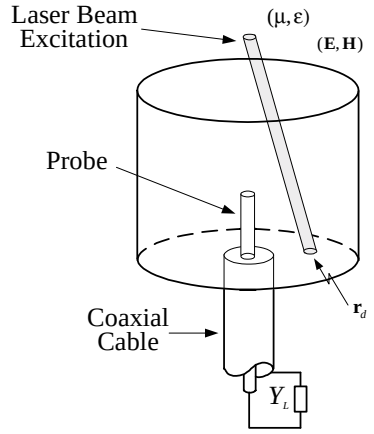

Figure 1. Probe in a metal can illuminated by a spot of a laser light.

coax and a signal is induced on the load admittance Y_L terminating the end of the coax remote from the point where it joins the bottom of the can. It is this signal at a $50\,\Omega$ load ($50\,\Omega$ coax assumed), as a function of the laser beam characteristics, that one wishes to determine. For a vanishingly small spot of laser light on the conducting surface, the radiating source is modeled as an electric dipole normal to and located at the surface. For a larger spot, the source is taken to be an ensemble of normal dipoles whose amplitudes and phases are dictated by the characteristics of the laser light and the spot. In this work we only consider the small-spot case. The extension to the larger spot is trivial as the spot is modeled by dipoles with known phase and amplitude distribution on the surface.

The dipoles radiate in the presence of the entire can-coax structure and, therefore, all parts of the can and coax, together with the terminating load, must be accounted for simultaneously in any analysis for determining the voltage at the load Y_L. In other words, all parts of the structure are coupled and each influence the current induced on all surfaces. The direct approach to solving this problem would be to determine the radiation due to the elementary dipole on the surface and employ the electric field of this radiation as the excitation of an integral equation for the current on the can and the monopole. The integral equation must account for the load at the terminal end of the coax and its effect at the annular aperture formed where the coax joins the can bottom. And the coupling into the coax must be computed in order to arrive at a full account of the coax and its terminal load. The current induced on the can and the monopole surfaces would be a vector

surface density so the integral equation must be a vector equation. Fortunately, since one needs to know the signal only at the load, which electromagnetically speaking occupies a vanishingly small region of space, one can obtain the desired information by solving a radiation problem and employing the reciprocity theorem. This is far simpler than it would be to solve the reception problem directly in which one must allow the laser- stimulated dipoles to radiate in the presence of the loaded (load admittance Y_L in place at the end of the coax) coax-can structure. The indirect approach adopted here takes advantage of the reciprocity theorem and allows one to determine the signal at the coax terminal load from knowledge of the field radiated by the monopole-can structure under the condition that the excitation results from a current generator impressed at the terminal end of the coax. This scheme necessitates the formulation and solution of a simpler integral equation. It is simpler for two reasons. First, the integral equation is not a vector equation as it would be if the direct procedure were followed and, second, the equation and its unknown possess rotational symmetry since the can and the center-joined coax form a circularly symmetric structure, the field radiated by the structure due to excitation at the coax terminal is circularly symmetric. One might designate this procedure *indirect* but it allows one to obtain the desired signal far more efficiently than would a more direct method necessitating the solution of a vector integral equation rather than the scalar equation of the indirect procedure. The indirect approach, though far less complex than the direct, does not sacrifice rigor.

The solution of the problem of determining the signal induced by a modulated laser beam at the load which terminates the coax of the coax-can structure, has been reduced to two steps: First is the computation of the electric field at points on the coax-can structure where the laser light might fall, caused by TEM excitation at the coax terminus, and second, is application of the reciprocity theorem to obtain the signal at Y_L caused by the laser light. From knowledge of this electric field, the value of the load admittance, and the value of the impressed source, one can determine the signal induced in the load impedance by invoking the reciprocity theorem. This technique, though simpler than the more direct method, is completely rigorous and involves no approximations not employed in the direct procedure.

2. THE RECIPROCITY APPROACH

In Fig. 2a is illustrated the coax-fed monopole mounted in the can, together with an elementary dipole of current moment $Il\delta(\boldsymbol{r} - \boldsymbol{r}_d)\hat{\boldsymbol{n}}$ located at point $\boldsymbol{r}_d$ in space on the can surface where Il is the dipole

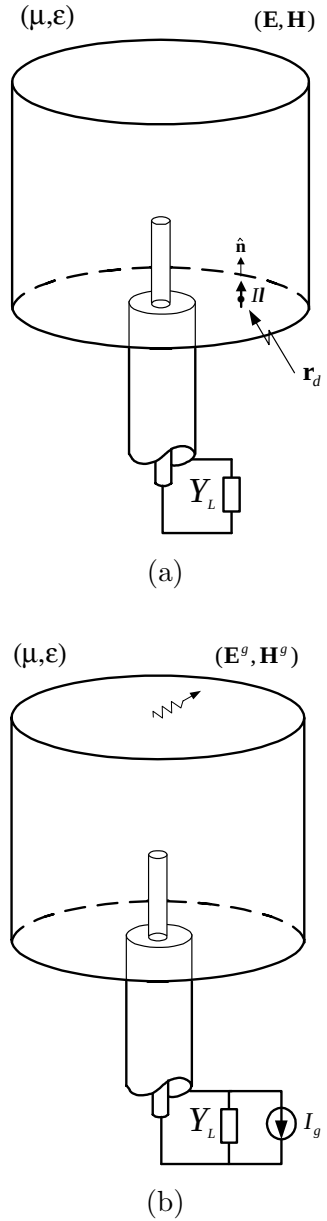

Figure 2. Reciprocity method applied to the original problem, (a) the original equivalent reception problem, (b) the radiation problem.

strength and $\hat{\boldsymbol{n}}$ is the unit normal for the can surface. An admittance Y_L terminates the end of the coax remote from the monopole and can. The dipoles radiate a field that couples with the can and the monopole terminated in the loaded coax, ultimately causing a signal to appear across Y_L. To set the stage for the use of the reciprocity theorem, we now consider a second source and resulting radiated field. This source is an ideal current generator of I_g amperes impressed at the terminal end of the coax. This current generator, located very close to admittance Y_L, produces a signal in the coax, which, in turn, excites the monopole, and can and gives rise to a radiated field $\boldsymbol{E}^g$ as illustrated in Fig. 2b.

A possible structural form that this generator and Y_L may take is illustrated in Fig. 3a. Notice that a shorted quarter wave transmission line is added at the load at $z = z_g$, because the reciprocity integrals must be evaluated at a closed surface. The transmission line model of this structure and its equivalent circuit are shown in Fig. 3b. We let the generator current be a volume current of density

$$\boldsymbol{J}^g = -\delta(z - z_g)[I^g/2\pi\rho]\hat{\boldsymbol{\rho}} \tag{1}$$

impressed at the end of the coax immediately adjacent to the admittance fabricated in annular form. The current generator is impressed at position $z = z_g$ along the coax. The negative sign on the current simply implies that the current is directed radially inward.

To apply reciprocity, it is instructive to think of two situations or two experiments. In the first, the impressed generator current I_g is turned off (leaving an open circuit) and the dipole on the conducting surface radiates a field causing a voltage $\boldsymbol{\mathcal{V}}$ to appear across the coax at the location of the generator and load admittance Y_L as seen in Fig. 2a. Next, the dipole is removed and the current generator turned on as in Fig. 2b. It excites the coax fed monopole and can and causes a field to be radiated, whose electric field is designated $\boldsymbol{E}^g$. The reciprocity theorem applied to these sources and fields can be stated in the form

$$\iiint_V (\boldsymbol{E}^g \cdot \boldsymbol{J} - \boldsymbol{E} \cdot \boldsymbol{J}^g) d = \oiint_S (\boldsymbol{E}^g \times \boldsymbol{H} - \boldsymbol{E} \times \boldsymbol{H}^g) \cdot \hat{\boldsymbol{n}} dS \tag{2}$$

where V is the region in which the theorem applies and S is the closed surface bounding this region. $\boldsymbol{J}^g$ and $\boldsymbol{J}$ are sources which acting alone produce fields $(\boldsymbol{E}^g, \boldsymbol{H}^g)$ and $(\boldsymbol{E}, \boldsymbol{H})$, respectively [4]. For our case, V is defined to be the volume inside the coax, the body of the can, outside the wire probe (and the center conductor of coax), and inside the (imaginary) sphere at infinity. Let $S = S_\infty + S_{pec}$, where S_∞ is the sphere at infinity and S_{pec} is the remainder of S. Since this antenna

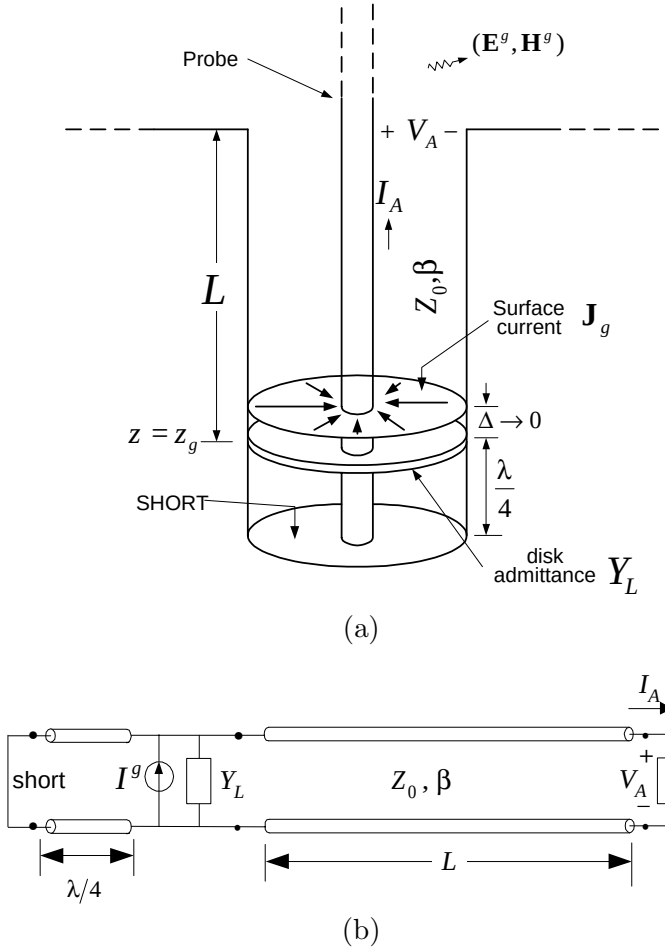

Figure 3. (a) A possible form of the generator and transmission line, (b) equivalent circuit.

structure is a perfect conductor, the surface integral over its surface S_{pec} is zero, and, due to the radiation condition, the integral over the sphere at infinity S_∞ is zero too. Hence, the surface integral of (2) is zero and one has remaining

$$\iiint_V (\boldsymbol{E}^g \cdot \boldsymbol{J} - \boldsymbol{E} \cdot \boldsymbol{J}^g) dV = 0 \tag{3}$$

where $\boldsymbol{E}$ is the electric field caused (everywhere) by the elementary dipole $\boldsymbol{J} = Il\delta(\boldsymbol{r} - \boldsymbol{r}_d)\hat{\boldsymbol{n}}$ radiating in the presence of the structure and

$\boldsymbol{J}^g$ is given by (1). Next we evaluate the integrals of (2). The first term of (3) is evaluated as

$$\iiint_V \boldsymbol{E}^g \cdot \boldsymbol{J} dV = \iiint_V \boldsymbol{E}^g \cdot Il \left[\hat{l}\delta(\boldsymbol{r} - \boldsymbol{r}_d)\right] dV = Il\hat{\boldsymbol{n}} \cdot \boldsymbol{E}^g(\boldsymbol{r}_d). \quad (4)$$

The coax is operated in its typical way in which all higher order modes are below cutoff. Thus, the fields and currents in the coax are circularly symmetric which implies that $\boldsymbol{E}$ is independent of ϕ. Since $\boldsymbol{J}^g$ is an annular current concentrated at $z = z_g$, the second term of (3) simplifies immediately to

$$\iiint_V \boldsymbol{E} \cdot \boldsymbol{J}^g dV = -I_g \int_{-\pi}^{\pi} \int_a^b \frac{1}{2\pi\rho} \hat{\boldsymbol{\rho}} \cdot \boldsymbol{E}(\rho, z_g) \rho d\rho d\phi = -I_g \boldsymbol{\mathcal{V}} \quad (5)$$

where $\boldsymbol{\mathcal{V}}$ is the potential of the coax center conductor relative to that of the outer conductor:

$$-\boldsymbol{\mathcal{V}} = -\int_a^b E_\rho(\rho, z_g) d\rho. \quad (6)$$

From (4) and (5) it is clear that one can obtain $\boldsymbol{\mathcal{V}}$, the voltage created across the coax by the dipole with the current generator off, from knowledge of the position and orientation of laser-induced dipole and the electric field $\boldsymbol{E}^g$ which results from the current generator applied at the coax terminus. Finally we apply reciprocity by replacing the integrals of (3) by their equivalent expressions from (4) and (5) to obtain

$$\boldsymbol{\mathcal{V}} = -Il\hat{\boldsymbol{n}} \cdot \boldsymbol{E}^g(\boldsymbol{r}_d)/I_g. \quad (7)$$

The procedure for using reciprocity is outlined as follows. First, one assumes a voltage $V_A = 1$ volt across the coaxial aperture and computes the current on the monopole and can. From knowledge of this current, driven by a one-volt generator ($V_A = 1$ volt), one can compute the driving-point or input admittance Y_A at the base of the monopole. This is the admittance "seen" by the coax where it joins the can. Since the monopole is driven by the coax, Y_A serves as the terminating admittance of the end of the coax where its center conductor becomes the monopole. Second, one determines the currents on the monopole and can and the field radiated by the structure under the condition that it is excited by the current generator through the coaxial line as illustrated in Fig. 3a. From transmission line theory, it is obvious that the current generator of Fig. 3b causes the voltage V_A in the coaxial aperture at the base of the monopole to be

$$V_A = \frac{(1 + \Gamma_A)e^{-j\beta L}}{Y_L\left(1 + \Gamma_A e^{-j2\beta L}\right) + Y_0\left(1 - \Gamma_A e^{-j2\beta L}\right)} I_g \quad (8)$$

in which β is the propagation factor of the line. Γ_A is the reflection coefficient at the monopole base

$$\Gamma_A = \frac{Y_0 - Y_A}{Y_0 + Y_A} \tag{9}$$

and Y_0 is the characteristic admittance of the line. V_A of (8) is the actual voltage driving the monopole so one can now compute the actual currents on the structure and, subsequently, the radiated field caused by the current generator in the coax. This is done by the procedure used to compute the currents with $V_A = 1$ volt or one can simply scale all current and field values by the ratio $V_A : 1$. The last step is to compute the voltage $\boldsymbol{\mathcal{V}}$ across the load Y_L from (3). The value of the voltage $\boldsymbol{\mathcal{V}}$ across Y_L due to the dipole moment Il at $\boldsymbol{r}_d$ is obtained form

$$\frac{\boldsymbol{\mathcal{V}}}{Il} = -\hat{\boldsymbol{n}} \cdot \boldsymbol{E}^g(\boldsymbol{r}_d) \frac{(1+\Gamma_A)e^{-j\beta L}}{V_A\left[Y_L(1+\Gamma_A e^{-j2\beta L}) + Y_0(1-\Gamma_A e^{-j2\beta L})\right]}. \tag{10}$$

The value computed for $\boldsymbol{\mathcal{V}}$ depends on the dipole moment $Il\hat{\boldsymbol{n}}$ of the dipole induced on the structure surface at $\boldsymbol{r}_d$ and the current I_g of the current generator employed in the reciprocity procedure. Recall that $\boldsymbol{E}^g(\boldsymbol{r}_d)$ is the E-field radiated by the structure when the monopole is driven by the current generator through the coaxial transmission line. It is of interest to note that the magnitude of the voltage $|\boldsymbol{\mathcal{V}}/Il|$ at the load Y_L is independent of the length L of the coaxial line when the load matches the characteristic admittance Y_0 of the coax, i.e., when $Y_L = Y_0$.

3. INTEGRAL EQUATION AND NUMERICAL SCHEME

Since many antennas are rotationally symmetric and fed at their symmetry axis by coaxial probes through either an infinite or finite ground planes, it is important to have reliable methods to accurately predict the input impedance of such structures. We obtain in this section an electric field integral equation (EFIE) and solve it numerically by the Method of Moments [5, 6]. The monopole and the "can" have been considered as parts of a whole BOR. The coaxial aperture of the wire/BOR geometry is shorted, and a magnetic frill source is placed [7–9]. The frill field is then used as the excitation of the integral equation.

EFIE: Consider a perfect electrical conductor (pec) body in an infinite homogeneous space with surface S. An electric field $\boldsymbol{E}^i$, is incident on the body and induces a surface current $\boldsymbol{J}$ on S. This

current in turn radiates a scattered electric field $\boldsymbol{E}^s$. The fields must satisfy

$$[\boldsymbol{E}^s(\boldsymbol{r}) + \boldsymbol{E}^i(\boldsymbol{r})]_{\tan} = \boldsymbol{0}, \quad \boldsymbol{r} \in S, \tag{11}$$

on the conducting surface where "tan" denotes the tangential component of the field on S. An EFIE can be formulated to determine the induced electric current on the scatterer:

$$-j\frac{\eta}{k}\left\{k^2 \iint\limits_S \boldsymbol{J}(\boldsymbol{r}')G(\boldsymbol{r},\boldsymbol{r}')dS' + \nabla \iint\limits_S \nabla'_s \cdot \boldsymbol{J}(\boldsymbol{r}')G(\boldsymbol{r},\boldsymbol{r}')dS'\right\}_{\tan} = -\boldsymbol{E}^i_{\tan}(\boldsymbol{r}), \ \boldsymbol{r} \in S. \tag{12}$$

in which the free space Greens function is defined as

$$G(\boldsymbol{r},\boldsymbol{r}') = \frac{e^{-jk|\boldsymbol{r}-\boldsymbol{r}'|}}{4\pi|\boldsymbol{r}-\boldsymbol{r}'|}, \tag{13}$$

with $\eta = \sqrt{\mu/\varepsilon}$, and $k = \omega\sqrt{\mu\varepsilon}$. Let S be the surface of a BOR formed by rotating a 'generating arc', around the z-axis as shown in Fig. 4a. Assume that the excitation is of the form

$$\boldsymbol{E}^i = E^i_\rho(\rho,z)\hat{\boldsymbol{\rho}} + E^i_z(\rho,z)\hat{\boldsymbol{z}} \tag{14}$$

with $E^i_\phi = 0$. Under the condition imposed upon the excitation, the current induced on the BOR has a component only in the t direction

$$\boldsymbol{J}(t) = J_t(t)\hat{\boldsymbol{t}} \tag{15}$$

and the resulting scattered electric field has no ϕ component. The surface divergence and gradient operators are given by

$$\nabla_s \cdot \boldsymbol{J} = \frac{1}{\rho}\frac{\partial}{\partial t}(\rho J_t) \tag{16}$$

$$\nabla_s f = \hat{\boldsymbol{t}}\frac{\partial}{\partial t}f \tag{17}$$

on the BOR surface, allowing one to write (12) as

$$-j\frac{\eta}{k}\left\{k^2 \iint\limits_S J_t(t')\hat{\boldsymbol{t}}\cdot\hat{\boldsymbol{t}}'G(t,\phi;t',\phi')dS' + \frac{\partial}{\partial t}\iint\limits_S \frac{1}{\rho'}\frac{\partial}{\partial t'}(\rho' J_t(t'))G(t,\phi;t',\phi')dS'\right\} = -\boldsymbol{E}^i(\boldsymbol{r})\cdot\hat{\boldsymbol{t}}, \ \boldsymbol{r} \in S. \tag{18}$$

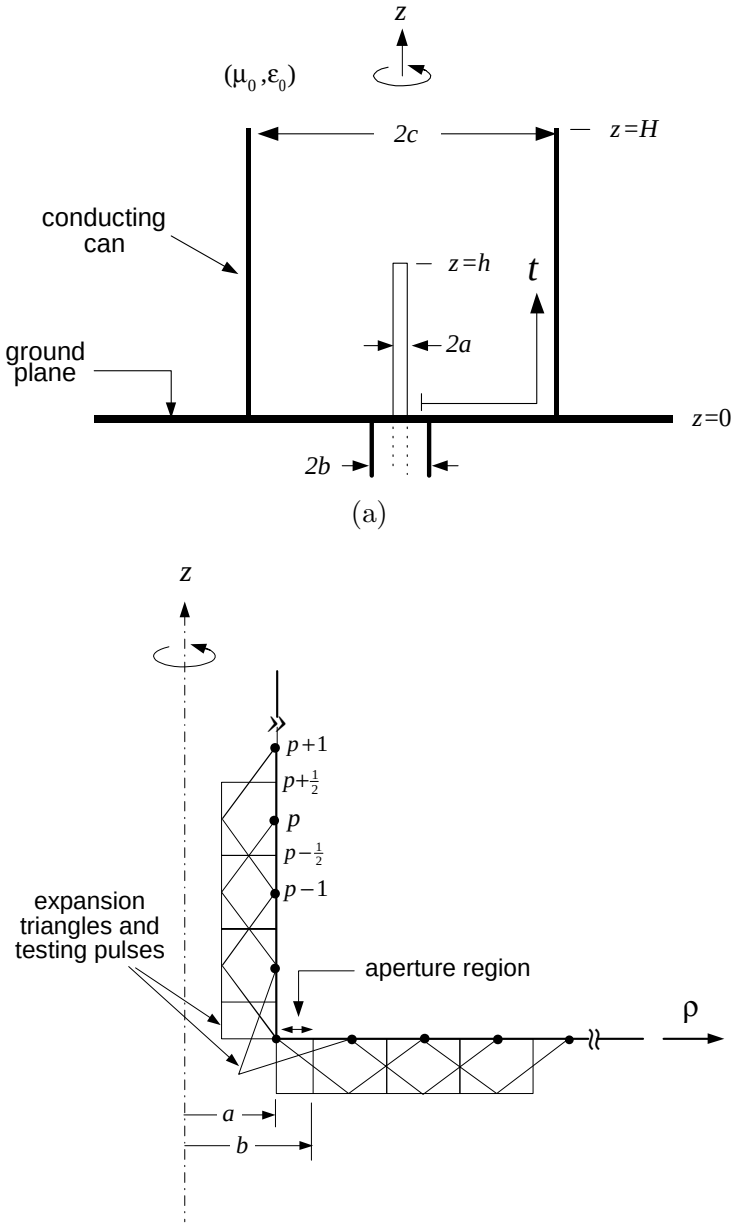

Figure 4. The coax-can mounted on a ground plane, (a) the parameters and (b) its numerical model.

Since all of the quantities of interest are independent of ϕ, one can set ϕ equal to some convenient value without affecting the value of the quantity. We select $\phi = 0$. Since

$$\hat{\boldsymbol{t}} = \sin\gamma\hat{\rho} + \cos\gamma\hat{\boldsymbol{z}}, \tag{19}$$

the dot product $\hat{\boldsymbol{t}}\cdot\hat{\boldsymbol{t}}'$ in (18) can be performed, and (18) can be rewritten as

$$-j\frac{\eta}{4\pi k}\left\{k^2\int_0^T I_t(t')\left[\sin\gamma\sin\gamma' K_1(t;t') + \cos\gamma\cos\gamma' K(t;t')\right]dt' + \frac{\partial}{\partial t}\int_0^T \frac{\partial}{\partial t'}I_t(t')K(t;t')dt'\right\} = -E_t^i(t),\ t\in(0,T) \tag{20}$$

where $I_t(t) = 2\pi\rho J_t(t)$, is the total current and K_1 and K are defined by

$$K_1(t;t') = \frac{1}{2\pi}\int_{-\pi}^{\pi}\frac{e^{-jkR}\cos\phi'}{R}d\phi', \tag{21}$$

and

$$K(t;t') = \frac{1}{2\pi}\int_{-\pi}^{\pi}\frac{e^{-jkR}}{R}d\phi', \tag{22}$$

in which

$$R = \sqrt{(\rho-\rho')^2 + (z-z')^2 + 4\rho\rho'\sin^2(\phi'/2)}. \tag{23}$$

In (20), T is the total arc length of the generating arc and ρ is the radial displacement, parallel to the xy or $\rho\phi$ plane, from the BOR axis (z-axis) to the general coordinate point (t,ϕ) on the surface of the BOR. γ and γ' are defined as the angles between the BOR axis and the unit vectors $\hat{\boldsymbol{t}}$ and $\hat{\boldsymbol{t}}'$, respectively.

Numerical Scheme: On the generating arc, $N+2$ points are defined, beginning with t_0 and ending with t_{N+1}, where the point identified by t_p is at arc displacement $t = t_p$, measured along the arc from the reference at $t = t_0 = 0$. We require $t_0 < t_1 < t_2 \ldots t_{N-1} < t_N < t_{N+1}$ in our point identification scheme, which enables one to define positive arc displacement in terms of a progression from lower to higher index number p of t_p. A simple piecewise-straight-line approximation to the generating arc is obtained by connecting t_0 to t_1, t_1 to $t_2,\ldots,t_p$ to $t_{p+1},\ldots,t_N$ to t_{N+1} with line segments. The arc displacement t_p, $p = 0,1,2,\ldots,N+1$, or the corresponding coordinate values (ρ_p, z_p), define a discretized piecewise linear approximation to

the surface of the BOR. It is this set of coordinate values (ρ_p, z_p), $p = 0, 1, 2, \ldots, N+1$, that serves as input of geometrical information to the numerical solution technique. The midpoints of the p^{th} and $(p+1)^{th}$ line segments are designated $t_{p-\frac{1}{2}}$ and $t_{p+\frac{1}{2}}$. The coordinates $(\rho_{p\pm\frac{1}{2}}, z_{p\pm\frac{1}{2}})$ corresponding to values of arc displacement $t_{p\pm\frac{1}{2}}$ along the discretized generating arc are not among the input data but can be determined from $\rho_{p\pm\frac{1}{2}} = (\rho_{p\pm1} + \rho_p)/2$. In order to solve for the N unknown coefficients, the current I_t, which is the unknown quantity, is approximated by a linear combination of N piecewise linear basis functions (triangles). The linear expansion coefficients are substituted into (20) and the equation is tested with a pulse function centered at t_m. This procedure leads to the following set of linear algebraic equations

$$[Z_{mn}][I_n] = [V_m] \tag{24}$$

in which $\{I_n\}$ are the N unknown coefficients of the finite-series representation of $I_t(t)$ and $[Z_{mn}]$ is a matrix whose elements are

$$\begin{aligned} Z_{mn} \;=\; & -\frac{j\eta}{4\pi k}\left\{\frac{k^2}{2}\left(\Delta_{m^-}\cos\gamma_{m^-} + \Delta_{m^+}\cos\gamma_{m^+}\right)\right. \\ & \left(\cos\gamma_{n^-}\int_{t_{n-\frac{1}{2}}}^{t_n} K(t_m;t')dt' + \cos\gamma_{n^+}\int_{t_n}^{t_{n+\frac{1}{2}}} K(t_m;t')dt'\right) \\ & +\frac{k^2}{2}\left(\Delta_{m^-}\sin\gamma_{m^-} + \Delta_{m^+}\sin\gamma_{m^+}\right) \\ & \left(\sin\gamma_{n^-}\int_{t_{n-\frac{1}{2}}}^{t_n} K_1(t_m;t')dt' + \sin\gamma_{n^+}\int_{t_n}^{t_{n+\frac{1}{2}}} K_1(t_m;t')dt'\right) \\ & +\frac{1}{\Delta_{n^-}}\int_{t_{n-1}}^{t_n}\left[K(t_{m+\frac{1}{2}};t') - K(t_{m-\frac{1}{2}};t')\right]dt' \\ & \left.-\frac{1}{\Delta_{n^+}}\int_{t_n}^{t_{n+1}}\left[K(t_{m+\frac{1}{2}};t') - K(t_{m-\frac{1}{2}};t')\right]dt'\right\} \end{aligned} \tag{25}$$

where Δ_{p^-} is the length of the subsection extending from the $(p-1)^{th}$ subcontour endpoint to the p^{th} subcontour endpoint, Δ_{p^+} is the length of the subsection extending from the p^{th} subcontour endpoint to the $(p+1)^{th}$ subcontour endpoint, γ_{p^-} and γ_{p^+} are the angles between the BOR axis and the $(p-1)^{th}$ and $(p+1)^{th}$ subsections, respectively [5].

$[V_m]$ is a column vector whose elements are computed from

$$V_m = \int_{t_{m-\frac{1}{2}}}^{t_{m+\frac{1}{2}}} E_t^i(t_m)dt. \tag{26}$$

When obtaining the elements of $[V_m]$ from (26), the frill field is tested with pulses as shown in the numerical model Fig. 4b. The half pulse at $\rho = a$ and $\rho = b$ corresponds to the location of the aperture region. One can use more testing pulses in the aperture region depending on the electrical size of the coaxial aperture.

Lossy BOR: To formulate an EFIE to account for the losses on an imperfectly conducting BOR surface, the impedance boundary condition is applied

$$\left[\boldsymbol{E}^s(\boldsymbol{r}) + \boldsymbol{E}^i(\boldsymbol{r})\right]_{\tan} = \boldsymbol{J}(\boldsymbol{r})Z(\boldsymbol{r}), \quad \boldsymbol{r} \in S, \tag{27}$$

in which $Z(\boldsymbol{r})$ is the surface impedance profile of the body [10]. The integral equation in (20) is modified to account for this modification as

$$-j\frac{\eta}{4\pi k}\left\{k^2\int_0^T I_t(t')\left[\sin\gamma\sin\gamma' K_1(t;t') + \cos\gamma\cos\gamma' K(t;t')\right]dt' + \frac{\partial}{\partial t}\int_0^T \frac{\partial}{\partial t'} I_t(t')K(t;t')dt'\right\} - I_t(t)\frac{Z(t)}{2\pi\rho} = -E_t^i(t),\ t \in (0,T). \tag{28}$$

Computation of the Near Field: Computation of the near field on the antenna structure provides a direct means of ascertaining the accuracy of the integral equation solution since surface quantities can be measured. For instance, if a rotationally symmetric antenna is excited by a rotationally symmetric source, the total field everywhere is rotationally symmetric. In this case it is possible to probe the antenna surface without significantly affecting the field structure. So one can probe relative field strength at different locations on the antenna surface through a slot oriented in such a way that its presence does not modify the field from the slotless case. The charge density induced on the antenna surfaces can be related to components of electric field. These components can, in principle, be computed once the current and charge on the antenna are known. For rotationally symmetric antennas, which are excited by a coaxial probe at the center, the incident field is that due to the magnetic frill source in the coax aperture. The normal scattered field on the BOR surface is due to the induced current and charge. The total field is the sum of the incident and scattered fields, which can be computed from

$$\boldsymbol{E}(\boldsymbol{r}) \cdot \hat{\boldsymbol{n}} = [\boldsymbol{E}^i(\boldsymbol{r}) + \boldsymbol{E}^s(\boldsymbol{r})] \cdot \hat{\boldsymbol{n}}. \tag{29}$$

Equation (29) can be computed once the current and charge are known. The normal component of the incident electric field may be computed from the components of the frill field as

$$\hat{\boldsymbol{n}} \cdot \boldsymbol{E}^i = E^i_\rho(\rho, z) \cos\gamma - E^i_z(\rho, z) \sin\gamma. \tag{30}$$

4. EXPERIMENTAL APPARATUS AND MEASUREMENT

Measured data are taken when the coax-can structure is mounted on a ground plane to provide isolation of the device under test (DUT) from the instrumentation. In this case one can "access" the interior region of the can bottom through the ground plane without disturbing the original field structure as illustrated in Fig. 5a. The ground plane and can configuration allows one to employ image theory in the comparison of measured and computed data. When the operating frequency of the can is sufficiently below the cut-off frequency of the corresponding circular waveguide formed by the can, the interior fields decay sufficiently below cut-off, as a function of axial displacement away from the can end. The field that escapes the can is very small and does not couple significantly with exterior objects surrounding this experimental model. So there is no need for a ground plane in this measurement. For this case one can access the interior region of the can wall through a short section of an axially directed thin slot cut in the can wall without disturbing the field as suggested in Fig. 5b.

Construction of the can: A tapered edge circular brass disk of thickness 3/8 inch has been constructed. This disk serves as the can bottom and is machined to fit the mating receptacle in the ground plane. A tapered hole is drilled at the center of this circular disk for insertion of the coaxial monopole. A circumferential groove, approximately 1/8 inch deep and 14.55 cm inner diameter, is cut in the disk to receive the can wall. This slot was made slightly thicker than the thickness of the can wall to ensure a snug fit. Along a radial line from a point close to the hole at the center to a point very close to the can wall, a 1/16 inch wide radial slot was cut in the disk to allow access to the interior can bottom. Since the source (monopole) field inside the can is rotationally invariant, the current in the can bottom is radially directed and ϕ invariant. This allows one to cut a thin radially directed slot in the can bottom (disk) with no resulting disturbance to the disk current. Access to the cans interior region for probing the field can be gained through this radially directed thin slot, which does not significantly alter the field structure. The ρ-directed slot does not interfere with the ρ-directed current on the can interior bottom. A rectangular brass sheet of thickness 1/16 inch is

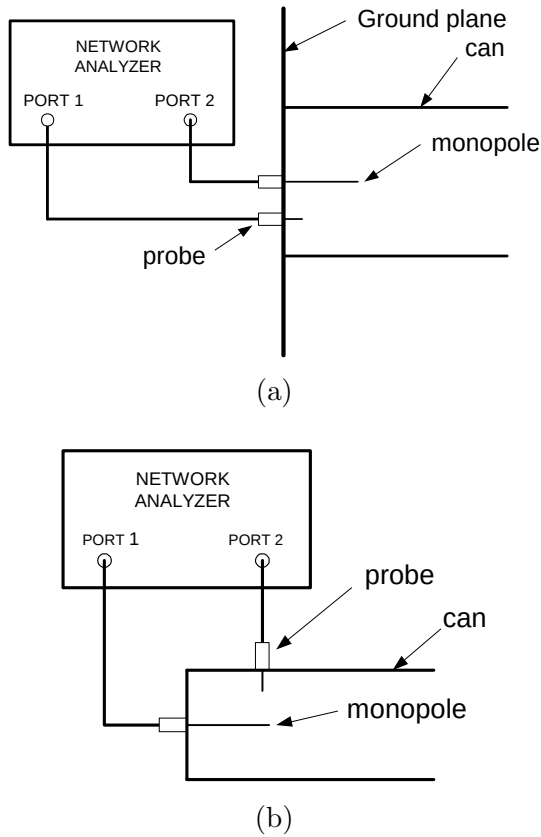

Figure 5. The measurement, (a) can bottom measurement, (b) can wall measurement.

rolled to construct the cylindrical can wall of inner radius 14.55 cm and approximate height of 15 inch. This cylindrical can wall is then inserted in the circumferential groove of the circular brass disk and soldered. The can wall is then soldered along the vertical joint with a copper strip applied for mechanical strength. The whole structure is then mounted on the ground plane.

For measuring the charge and current on the interior can wall below cut-off, the cylindrical brass tube of diameter 6.55 cm (can), the monopole, and the probes of [11] are assembled into an experimental model. Along the wall of this can a short thin slot has been cut parallel to the axis of the can (z-axis) to allow access to the interior can wall. Since the source (monopole) field inside the can is rotationally invariant the current in the can wall is axially directed and ϕ invariant. This

allows one to cut a thin z-directed slot in the can wall with no resulting disturbance to the wall current. Access to the cans interior region for probing the field can be gained through this z-directed thin slot, which does not significantly alter the field structure since the probe and z-directed slot do not interfere with the z-directed current on the can interior wall.

Construction of a charge probe and monopole: This probe is used for measuring the charge (or electric field normal to the surface, E_ρ and E_z). Since the charge probe must couple to the normal electric field, it is simply a very short monopole type probing element. The details on constructing a charge probe and monopole is readily available in [11]. The can, the monopole and the probes are finally assembled into an experimental configuration as shown in Fig. 5.

5. RESULTS AND CONCLUSION

Experimental and computed data are compared to enable us to demonstrate the validity of our work. Two types of comparative data are presented to lend plausibility to the validity of the theoretical and numerical aspects of this work. The first set of data is of driving-point admittance. The next data are of the values of relative field strength (referred to in the plots as the normalized electric fields) on the interior can bottom and can wall. The input impedance of the structures were calculated from the scattering parameter S_{11}. The measured S_{12} data is used for determining the relative charge. Measurements along the thin slots were made for a variety of antenna configurations and different monopole lengths. For the charge measurements, data have been taken over the frequency ranges of interest at increments of 0.5 cm along the radial slot at the can bottom while the data are taken at 1.0 cm increments along the axial slot. Since the absolute response of the specifically designed and constructed field probes were not known, the measured data were normalized by a complex constant at a specified frequency to facilitate comparison against the computed data. The comparative data presented in this section confirm the accuracy of the numerical solutions obtained in this work.

Shown in Fig. 6 are real and imaginary parts of the measured and computed driving-point admittance for a 13.1 cm long monopole antenna exciting the can over the frequency range from 300 MHz to 3000 MHz. The can is below cut-off when operated below 790 MHz. Because the can is operated below cutoff frequency of the TM_{01} mode of the corresponding circular waveguide, power cannot be delivered to the can by the monopole and the real part of the driving-point admittance is zero (at least for the computed part since loss effects are

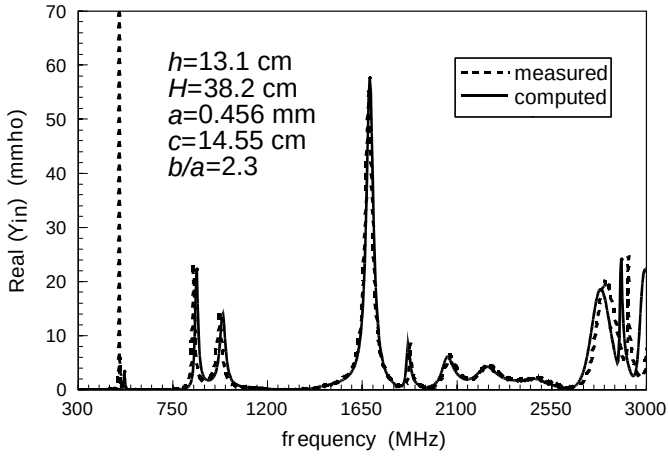

(a)

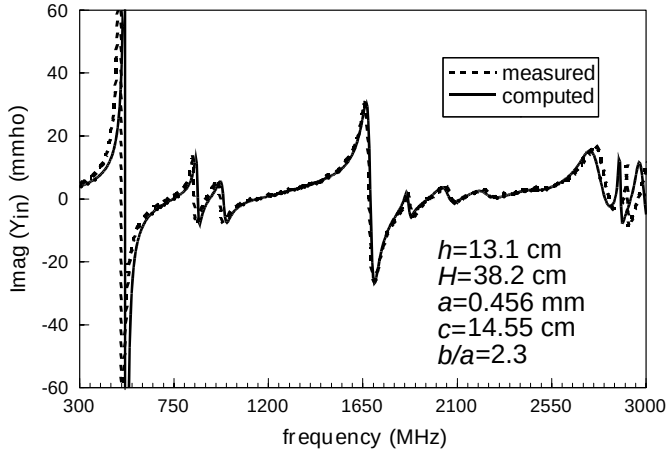

(b)

Figure 6. Input admittance of the lossless coax-can, (a) the real part (b) the imaginary part.

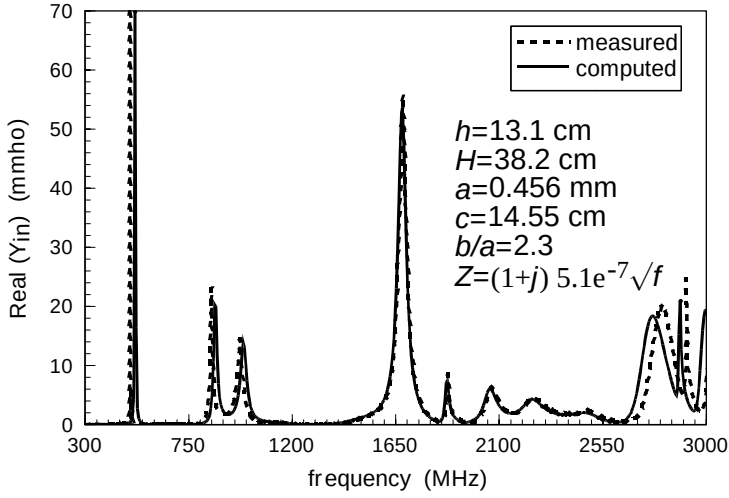

(a)

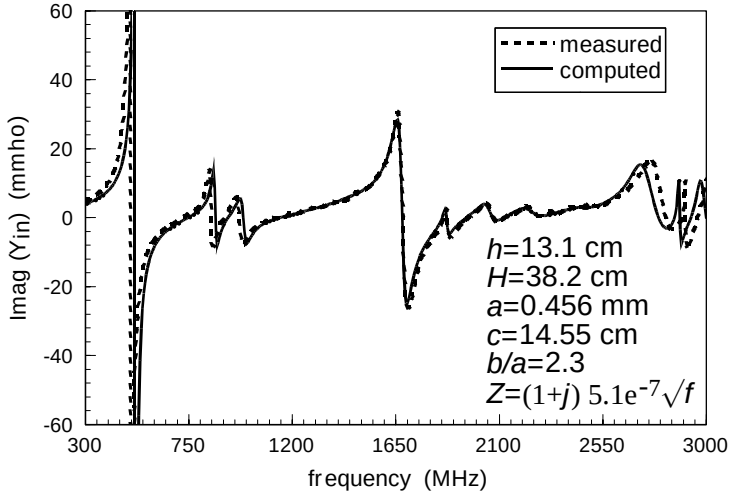

(b)

Figure 7. Input admittance of the lossy coax-can, (a) the real part (b) the imaginary part.

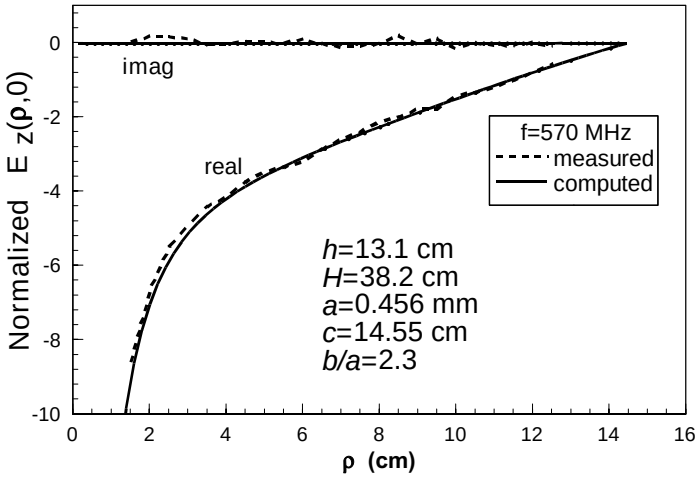
imag
real
f=570 MHz
measured
computed
h=13.1 cm
H=38.2 cm
a=0.456 mm
c=14.55 cm
b/a=2.3
Normalized E z(ρ,0)
ρ (cm)
0
-2
-4
-6
-8
-10
0
2
4
6
8
10
12
14
16

(a)

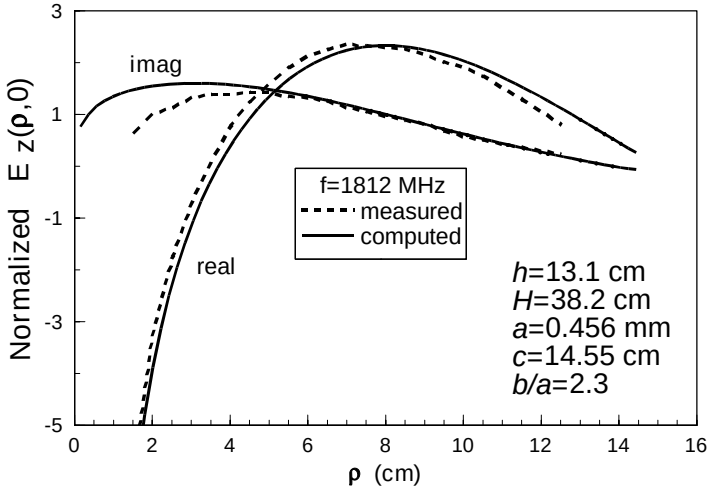
imag
real
f=1812 MHz
measured
computed
h=13.1 cm
H=38.2 cm
a=0.456 mm
c=14.55 cm
b/a=2.3
Normalized E z(ρ,0)
ρ (cm)
3
1
-1
-3
-5
0
2
4
6
8
10
12
14
16

(b)

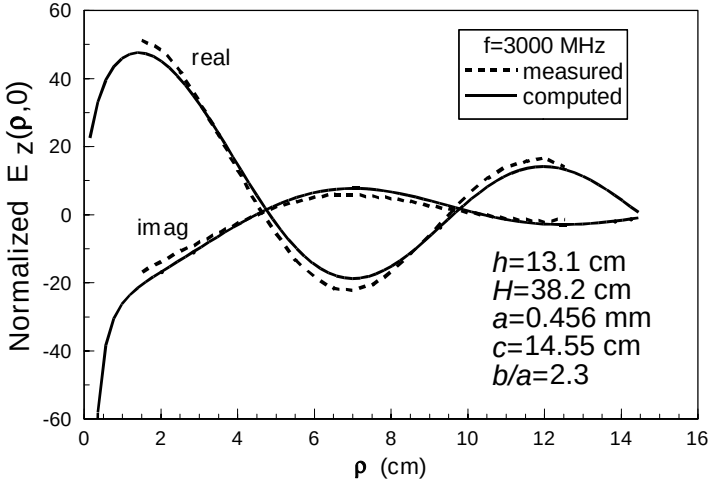

(c)

Figure 8. The computed and measured values of the normal electric field (charge) at the can bottom for, (a) 570 MHz, (b) 1812 MHz, and (c) 3000 MHz.

not modeled). Since appreciable power cannot escape the structure excited by the monopole antenna operating below cutoff, the monopole must present a purely reactive load to the generator.

The measured real part of input admittance in a very narrow band about 469 MHz is very large relative to that at other frequencies, even though this frequency is below the cut-off frequency (790 MHz). The computed value of this real input admittance is very small and is quite different from the measured. This divergence of measured and computed values is expected and explainable. Since this operating frequency is below cut-off, no appreciable energy should leak from the can, which observation appears inconsistent with the significant value of real Y_{in}, which implies that power is being supplied to the monopole. At 469 MHz, the monopole and its image effectively form a straight segment which is $\lambda/2$ long. Under this condition the monopole is resonant and its current is very large. This very large current strongly excites the can and, hence, the losses in the monopole and can are much greater than at other non-resonant frequencies. The large real Y_{in} is, indeed, consistent with significant power delivered through the monopole to supply the losses experienced in the finitely conducting material from which the can and monopole are fabricated. The computed values of real Y_{in} do not exhibit this behavior because

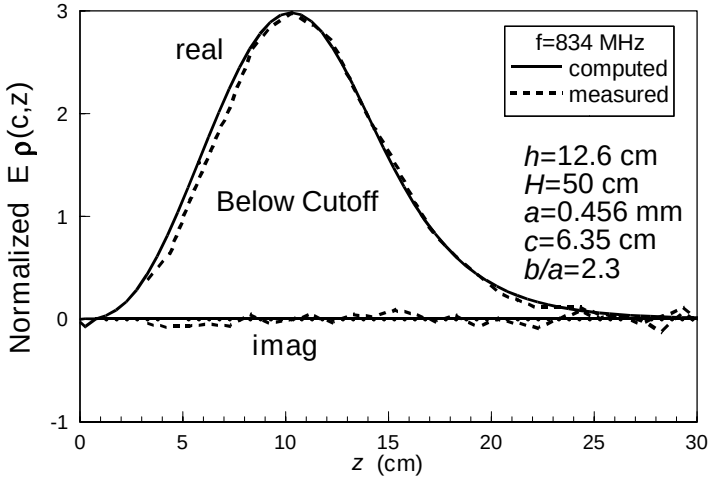
real
f=834 MHz
computed
measured
Below Cutoff
h=12.6 cm
H=50 cm
a=0.456 mm
c=6.35 cm
b/a=2.3
imag
Normalized E ρ(c,z)
z (cm)

(a)

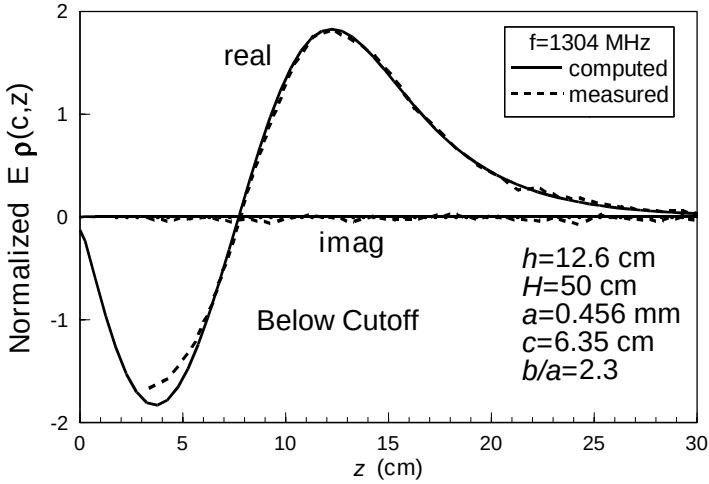
real
f=1304 MHz
computed
measured
imag
h=12.6 cm
H=50 cm
a=0.456 mm
c=6.35 cm
b/a=2.3
Below Cutoff
Normalized E ρ(c,z)
z (cm)

(b)

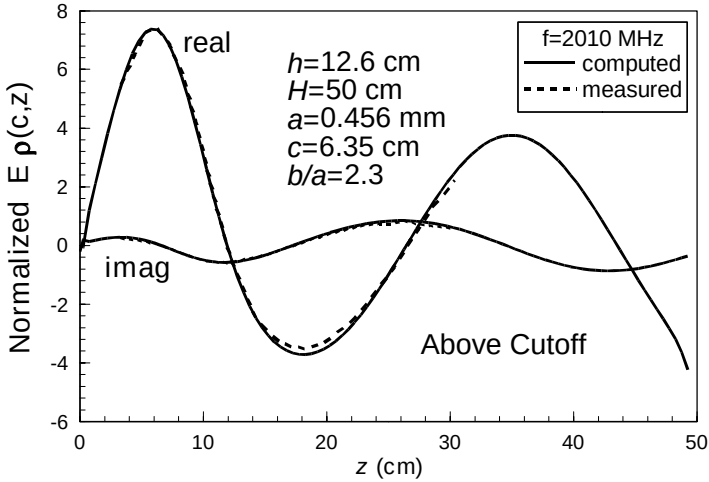

(c)

Figure 9. The computed and measured values of the normal electric field (charge) at the can wall for, (a) 570 MHz, (b) 1812 MHz, and (c) 3000 MHz.

the integral equation is formulated on the basis of the assumption that the monopole and can are perfect conductors and, therefore, are lossless. In Fig. 7 one finds, for the purpose of comparison, measured and computed input admittance of a monopole attached to the bottom of a brass can of Fig. 4a. Losses due to the finite conductivity of the brass are accounted for in the analysis by making use of the well-known surface impedance approximation. It has been ensured that the thickness of the walls of brass can used in this measurement is at least ten times greater than the skin depth at the frequency of operation.

In Fig. 8 are depicted real and imaginary parts of the measured and computed normalized axially directed electric field strengths at the bottom of the can along a line from the location of the coax center to the can wall. Since it is not feasible to calibrate the charge and current probes for absolute magnitude and phase, the measured data shown in these figures are normalized by a complex constant at a selected position along the radial slot. The basis of the normalization is that one assumes the measured and calculated values to be equal at a single point and then compares the two sets of data at other points along the range (displacement) of measurements. This normalization is done to aid the reader who wishes to compare measured and computed data.

In Fig. 9 are shown of real and imaginary parts of the measured

and computed ρ-directed electric field strengths at the inner surface of the can wall for the 12.6 cm long monopole antenna exciting the can at selected frequencies. The measured data shown in these figures are normalized by a complex constant so as to match the computed data along the slot. Notice that, since the can is operated below cut-off (1800 MHz), the actual data for the ρ-directed electric field should have zero imaginary part.

One concludes that the indirect method suggested above is rigorous, but less complex for determining the signal induced at the load due to the laser beam excitation of the coax-can structure. Of course one can determine the values needed in the reciprocity formula by some other methods. Finally, excellent agreement is achieved between computed and measured results in almost all cases. Where the agreement is only "good", explanations are offered.

ACKNOWLEDGMENT

The authors gratefully acknowledge the support of this work by the Air Force Office of the Scientific Research (AFOSR) through grant F49620-96-1-0005.

REFERENCES

1. Dudley, D. G. and K. F. Casey, "A measure of coupling efficiency for antenna penetrations," *IEEE Trans. Electromagnetic Comp.*, Vol. 33, No. 1, 1–9, Feb. 1991.
2. Qiu, Z. and C. M. Butler, "Analysis of a wire probe mounted on the nose of a missilelike body of revolution," *URSI National Meeting*, 11, Colorado, Boulder, 1994.
3. Ozzaim, C. and C. M. Butler, "Coupling to a probe in a metal can by an electric dipole," *IEEE Antennas Propagat. Symp. Digest*, 23–26, 1999.
4. Harrington, R. F., *Time Harmonic Electromagnetic Fields*, McGraw-Hill, New York, 1961.
5. Qiu, Z. and C. M. Butler, "Analysis of a wire in the presence of an open body of revolution," *Progress in Electromagnetic Research*, PIER-15, 3–26, 1997.
6. Harrington, R. F., *Field Computation by Moment Methods*, IEEE Press, Piscataway, NJ, 1993.
7. Butler, C. M. and L. L. Tsai, "An alternate frill field formulation," *IEEE Trans. Antennas Propagat.*, Vol. 21, No. 1, 11–16, Jan. 1973.

8. Tsai, L. L., "A numerical solution for the near and far fields of an annular ring of magnetic current," *IEEE Trans. Antennas Propagat.*, Vol. 20, No. 5, 569–576, Sep. 1972.
9. Junker, G. P., A. W. Glisson, and A. A. Kishk, "Accurate impedance model for antiresonant monopoles on finite ground planes," *Electronics Letters*, Vol. 32, No. 18, 1632–1633, Aug. 1996.
10. Rothwell, E. J. and M. J. Cloud, "A Hallen-type integral equation for symmetric scattering from lossy circular disks," *IEEE Trans. Antennas Propagat.*, Vol. 40, No. 8, 920–925, Aug. 1992.
11. Martin, A. Q. and C. M. Butler, "Corroboration of the analysis of an axially directed antenna exciting a conducting tube," *Journal of Electromagnetic Waves and Applications*, Vol. 11, 821–858, 1997.

Cengiz Ozzaim was born in Arhavi, Turkiye. He received the B.S. and M.S. degrees from Middle East Technical University, Ankara, in 1987 and 1991, respectively. He received the Ph.D. degree from Clemson University, SC, in 1999. From 1988 to 1993 he worked as an RF engineer in Turk Telekom, Ankara. From 1994 to 1999 he was research assistant at Clemson University. From 1999 to 2000 he worked as an antenna design engineer in Dayton-Granger, Ft. Lauderdale, FL. From 2000 to 2002 he worked as an RF engineer in DENSO International America LA Laboratories, Carlsbad, CA. Since 2002, he has been at Dumlupinar University, Kutahya where he is presently an assistant professor. His current research interests are computational electromagnetics, antennas, and RF circuit design.

Chalmers M. Butler received the B.S. and M.S. degrees from Clemson University, SC, and the Ph.D. degree from the University of Wisconsin, Madison. From 1965 to 1974, he was a Faculty Member with Louisiana State University, the University of Houston, and the University of Mississippi, where he was Chair of Electrical Engineering and University Distinguished Professor from 1976 to 1983. Since 1985, he has been at Clemson University, where he is presently Alumni Distinguished Professor. His research focus has been on integral equation techniques in electromagnetics and numerical methods for solving integral equations; he is also interested in antennas and aperture penetration.